

A High Spectral Resolution Atlas of Comet 122P/de Vico

Anita L. Cochran and William D. Cochran
Department of Astronomy and McDonald Observatory
University of Texas at Austin, Austin, TX
Accepted for publication in *Icarus*

Abstract

On 3 and 4 October, 1995, we obtained high spectral resolving power ($R = \lambda/\Delta\lambda = 60,000$) observations of comet 122P/de Vico using the 2DCoude cross-dispersed echelle spectrograph on the 2.7-m telescope of McDonald Observatory. The spectra cover the wavelength range from 3830Å–10192Å. The spectra from 3830–5776Å are continuous; from 5777–10192Å there are increasing interorder gaps. The comet was at a heliocentric distance of 0.66 AU and a geocentric distance of 1.0 AU. Comet de Vico has a very high gas-to-dust ratio and the spectra have excellent signal/noise. These two factors combined to yield spectra with a large number of emission lines. We have collected laboratory molecular line lists and have used these line lists in order to identify as many of the detected lines as possible. We have identified 12,219 emission lines and have located another 4,055 lines which we cannot identify. We present representative spectra and identifications along with a description of our plans to make these spectra and identifications available to the community. This atlas should prove a valuable tool for future studies of comets.

Keywords: comets, spectroscopy

1 Introduction

Understanding the physics and chemistry of comets can lead to significant improvements in our knowledge of the formation of the Solar System. Such studies allow constraints on the physical conditions in the solar nebula, on the dynamical evolution of the disk and of planetesimals, and on the chemical evolution of these bodies. High resolving power spectroscopic observations offer unique opportunities for studies of the origin and subsequent chemistry of comets. For example, measurement of atomic isotope ratios in a sample of “Kuiper belt” and “Oort cloud” comets can place valuable new constraints on physical processes in the solar nebula and proto-planetary disk during the comet formation epoch.

The complex molecular spectrum of the coma of a comet results in thousands of lines being visible in the spectral region from 3800–10200Å. In order to undertake studies of a particular feature or molecule, one must be able to identify most of the lines in the region of interest. Yet many spectral regions are complicated by the superposition of lines from more than one molecule. In addition, laboratory studies of diatomic and polyatomic molecules are often difficult to obtain and incomplete. Valk *et al.* (1992) published a catalogue of line identifications for the near-UV and blue region of the spectrum of Comet C/1989 X1 (Austin) from spectra at moderate spectral resolving power ($R=2,500$). Brown *et al.* (1996) published a catalog of cometary emission lines from comets 109P/Swift-Tuttle and C/1989 X1 (Austin). They found 2997 lines and were able to identify 2438 of them. Zhang *et al.* (2001) utilized high resolution spectra of C/1995 O1 (Hale-Bopp) and the catalogue of Brown *et al.* in order to identify 532 emission lines (73 unidentified). These catalogues are a critical first step for cometary science.

This paper represents an update to the catalogues of Brown *et al.* and Zhang *et al.* We present observations of comet 122P/de Vico obtained at McDonald Observatory in October 1995. Comet de Vico is the perfect target for such a study since it has a very high gas-to-dust ratio and was reasonably bright, allowing for spectra of exceptionally high signal/noise with very little continuum (signal/noise at peak was >300). We identified 12,219 lines in the spectrum of de Vico. In addition, there are 4,055 unidentified lines in our spectra.

2 Observations and Reductions

We observed comet 122P/de Vico with the 2.7-m Harlan Smith telescope of McDonald Observatory and the 2DCoude spectrograph (Tull *et al.* 1995) during October 1995 (see table I for information on the observations). These observations were obtained at a spectral resolving power of 60,000 and covered the wavelength range from 3800–5776Å continuously, with spectra with increasing interorder gaps from 5776–10192Å. Table II indicates the spectral coverage of each of the echelle orders. In all cases, the slit was 1.2 arcsec wide by 8.2 arcsec long. The spectra were extracted using variance weighting along the spatial dimension, with no attempt made to preserve spatial information. The signal/noise was extremely high throughout. De Vico represents a perfect comet for such identification work since the gas/dust ratio is one of the highest known for a comet. This results in spectra with almost no continuum so that even weak features are unambiguously

detected. In addition to spectra on the optocenter, we obtained one spectrum with the telescope offset 100 arcsec into the tail. These tail spectra are useful for distinguishing between neutral and ionized species.

Incandescent lamp spectra were obtained in order to flat field the data. The wavelength calibration was made by fitting a two-dimensional function to observations of a ThAr hollow-cathode lamp. Over 3100 lines were fit, with a fourth order fit along an order and fifth order fit across orders, resulting in an rms error of the wavelength of $\sim 2.5\text{m}\text{\AA}$. This is comparable to, or better than, typical laboratory spectra described in this paper. The cometary spectra were Doppler-shifted by a velocity equal to the geocentric radial velocity of the comet (i.e by $-\dot{\Delta}$ from table I to bring them onto the laboratory rest frame).

A cometary spectrum consists of molecular and atomic emission lines, superimposed on a continuum which results from sunlight reflecting off the dust. It is necessary to remove the underlying continuum from the emission spectrum if the goal of a study of the spectra is to determine the amount of a particular gas. However, removal of the continuum is fraught with uncertainties in the color of the dust and in photon statistics. Thus, removal of the continuum can induce noise into spectra. Fortunately, comet de Vico has a high gas/dust and the continuum is essentially negligible at all wavelengths. Given this and the problems associated with continuum removal, we chose not to remove the continuum for our purposes in this paper of line identification. This results in an offset of the spectrum from zero (typically the continuum for de Vico was about 350 counts and the emission lines are many thousands of counts). The continuum can also result in the apparent diminution of the strengths of emission lines when they coincide with a solar absorption feature. This might result in our not detecting a very weak feature.

In addition to the underlying continuum spectrum, there is a superposition of a telluric spectrum onto the cometary spectrum. This spectrum consists of emissions due to metastable oxygen, sodium, OH and O₂ and absorption due to O₂ and H₂O. The telluric spectrum is at the rest frame of the Earth's atmosphere and is, therefore, shifted by $-\dot{\Delta}$ with respect to the cometary rest frame. Thus, we Doppler shifted by this same velocity the telluric emission line lists discussed in the next section to identify the telluric features present in the Doppler-shifted cometary spectra.

The telluric emission lines are generally narrow and only affect the wavelength at which they occur. The telluric absorption is a different problem entirely. In the regions of the strong absorptions, such as the O₂ "A" band or the 9300 \AA H₂O band, almost all photons entering the atmosphere are absorbed before they reach the telescope. Thus, even if a line at these wavelengths is excited in the cometary spectrum, we will not record the feature in our spectrograph. There is no way to remove the effect of these saturated telluric absorptions and the information from the comet is forever lost (unless a spectrum taken at a different time has a Doppler shift that moves the cometary line and the telluric absorption apart). The orders most affected by the telluric absorption are orders 50 (O₂ "B" band), 48 and 47 (H₂O "a" band), 45 (O₂ "A" band), 42 and 41 (H₂O "z" band), and 38–35 (H₂O " γ " and " ρ " bands).

3 Linelists

One of the most difficult aspects of compiling a cometary spectral atlas is finding good laboratory line lists of all of the relevant molecules. As a first step in building our spectral atlas, we searched out many molecular line lists. Many of the molecules of importance were studied years ago and the line lists do not exist in digital form; we have spent many hours scanning line lists and typing in and checking large quantities of numbers by hand (possibly with undetected errors introduced). Some of the relevant molecules are not well understood and there are many unassigned lines. For some molecules, we have used work by several different authors to be as complete as possible. In the case of some molecules, such as CN, we had access to line lists which were much more inclusive than necessary. The tables of the identified molecular lines which we include as part of this paper list only those lines which we believe we detected. However, such over-complete line lists may prove useful for future cometary spectra. We note, also, that in the red and near-IR, there are interorder gaps in our data. In these regions, we leave gaps in the lists of identified lines. Refer to table II for a complete list of the wavelengths for which we have observations.

3.1 C₂

There are two principal band systems of C₂ which are observed in the optical in the spectra of comets. These are the Swan, or d³Π_g – a³Π_u, system, and the Phillips, or A¹Π_u – X¹Σ_g⁺, system. The Swan system is dominant in the green, orange and red region of the spectrum, while the Phillips is important in the near-IR and IR.

For the Swan system, we used the line list of Phillips and Davis (1968). We extended this line list for high J-values of the 0–0, 0–1 and 2–1 bands using the wavelength spacing of the highest previously defined lines to identify which emission lines were the continuation of these bands. We derived slightly different wavelengths for four of the highest J-value lines of the R-branches of the 1–0 band than in the original reference ($\Delta\lambda = 0.042\text{--}0.076\text{\AA}$). Most of our extensions are in agreement with the additional wavelengths also derived by Brown *et al.* (1996), though we observed to higher J-levels for the 0–0 band.

For the Phillips system, we used the works of Ballik and Ramsay (1967) and Chauville *et al.* (1977).

3.2 C₃

The C₃ molecule was first observed in cometary spectra in 1882, although the species causing the emission feature in comets was unknown. It is difficult to study in the laboratory because it is relatively unstable. Thus, the molecule causing the emission lines was not identified until 1951. In cometary spectra, the important bands are known as the “4050-Å Group”, indicative of the peak of the spectrum. However, careful inspection of cometary spectra show that lines attributable to this band can be seen from approximately 3350Å to 4700Å, although the main part of the band

is between 3900 and 4140Å with a maximum at 4050Å and an additional (but not well identified) peak at 4300Å.

The structure of this molecular band is quite complex since the bending frequency of the lower state is small and there is a large Renner-Teller splitting. The band has been identified as a $A^1\Pi_u - X^1\Sigma_g^+$ electronic transition (Gausset *et al.*, 1965). R-branch bandheads at 4072Å and 4260Å can be assigned to the (1,0,0)–(1,0,0) and (0,0,0)–(1,0,0) bands respectively (Merer, 1967). The density of the lines results in a pseudocontinuum from C₃.

C₃ is a linear, symmetric molecule containing nuclei which are identical in mass. For all Σ states of the molecule, every second line is missing. In other states, one member of the e/f -parity doublet of each rotational level is missing, although all rotational levels are represented (Tokaryk and Chomiak, 1997).

Most of our line identifications come from Gausset *et al.* (1965), with additional identifications from Merer (1967) and Tokaryk and Chomiak (1997). Tokaryk and Chomiak argue convincingly that the (0,2,0)–(0,0,0) and (0,2,0)–(0,2,0) rotational assignments of Gausset *et al.* are in error. Thus, in the wavelength region from 3990–4019Å we have preferentially used the Tokaryk and Chomiak assignments. However, Tokaryk and Chomiak do not report rotational assignments for these bands outside this wavelength region, so we have continued to use the Gausset *et al.* assignments for these two bands at other wavelengths.

The combination of the complexity of the spectrum and the difficulty of studying this molecule in the laboratory has meant that the line identifications are far from complete and may not always be accurate. This is readily apparent at 3949Å where we observe an obvious C₃ bandhead which is not in the line lists cited here. The lines which are identified in this region arise from the (0,4,0) – (0,2,0) band Q-branch, but the line identifications of Gausset *et al.* do not include any assignments for the R- or P-branches. Balfour *et al.* (1994) have studied C₃ at these wavelengths and do indeed identify this bandhead as the R-branch of the (0,4,0) – (0,2,0) band and identify other lines in the region as from the P-branch. However, the Q-branch assignments of Balfour *et al.* disagree with those of Gausset *et al.* Tokaryk and Chomiak have pointed out that the Balfour *et al.* spectra are at much lower resolution than the other spectra and that Balfour *et al.* may not have been able to disentangle the superimposed bands. We have no basis for choosing between the various assignments. We have chosen to neglect the Balfour *et al.* assignments entirely based on the arguments of Tokaryk and Chomiak. However, it is reasonably certain that the unidentified lines near 3949Å are from the R-band of the (0,4,0) – (0,2,0) band.

We do not resolve cleanly the C₃ lines in our spectra. The outflow of the gas in the coma broadens the line sufficiently that even at 3× the resolution with R=180,000, a resolving power we used with comets Hyakutake and Hale-Bopp, the C₃ is not resolved in the densest regions. Thus, we have not always been able to definitively match a line list with our spectra. In the densest regions, we have just assumed that all known lines were observed. There are some known lines (e.g. in the (0,0,0)–(0,4,0) or (0,0,0)–(0,6,0) bands) which we definitely *do not* observe in our spectra.

3.3 CH

A wonderful new, inclusive line list has recently become available for studies of CH. This is the SCAN-CH list of Jørgensen *et al.* (1996). This list includes transitions of $^{12}\text{C}^1\text{H}$ and $^{13}\text{C}^1\text{H}$ for the infrared transition $\text{X}^2\Pi - \text{X}^2\Pi$ and three electronic transitions $\text{A}^2\Delta - \text{X}^2\Pi$, $\text{B}^2\Sigma^- - \text{X}^2\Pi$, and $\text{C}^2\Sigma^+ - \text{X}^2\Pi$. A total of 112,821 lines are given for each isotope! We identified low-J lines of the 0–0 band of the B–X transition around 3900Å (some of which can be confused with isotopic lines of CN) and low-J lines of the 0–0 and 1–1 bands of the A–X transition around 4300Å. This new SCAN-CH line list includes the satellite transitions of the CH bands, which are observed in our spectra.

3.4 CN

Great effort has been expended to understand the CN molecule because it is a significant source of opacity in some stars. Thus, there are CN line lists which are much more inclusive than what is needed for cometary studies, where depopulation of the upper J-levels is relatively rapid.

Two different electronic band systems are seen in cometary spectra, the so-called violet system, or the $\text{B}^2\Sigma^+ - \text{X}^2\Sigma^+$ band, and the so-called red system, or the $\text{A}^2\Pi - \text{X}^2\Sigma^+$ band.

For the violet system, we used the line list of Kurucz (1995, CDRom 18) which contains about 350,000 lines. Lines of both $^{12}\text{C}^{14}\text{N}$ and $^{13}\text{C}^{14}\text{N}$ are included with J up to 150.5. For our purposes, we have only used the $^{12}\text{C}^{14}\text{N}$ wavelengths. Indeed, some of our “unidentified” lines may be lines of $^{13}\text{C}^{14}\text{N}$. Since this band is a $\Sigma - \Sigma$ transition, there are P- and R-branches but no Q-branch.

For the red system, we used the line list of Davis and Phillips (1963). Jørgensen and Larsson (1990) recently calculated CN red line lists with up to 1 million lines for $^{12}\text{C}^{14}\text{N}$. However, the Jørgensen and Larsson work is most concerned with completeness for line blanketing and is not derived from measured line positions. Thus, some of the line center uncertainties in this list are higher than we preferred, which is why we used the older reference.

3.5 NH₂

Throughout much of the red region of a cometary spectrum, there are scattered emission lines which are attributable to NH₂. The transitions responsible for these lines are the $\tilde{\text{A}}^2\text{A}_1 - \tilde{\text{X}}^2\text{B}_1$ electronic transition along with transitions between the high vibronic levels and the ground state of the $\tilde{\text{X}}^2\text{B}_1$ electronic band (e.g. $(0,13,0)\tilde{\text{X}}^2\text{B}_1 - (0,0,0)\tilde{\text{X}}^2\text{B}_1$). The spectrum of the NH₂ band is quite complex and irregular because the upper level is linear and the lower level is bent at an angle of 103°. Also, perturbations are important, as is the Renner-Teller effect.

The traditional reference for cometary NH₂ line lists is Dressler and Ramsay (1959). While this reference is moderately complete, it has been superseded in subsequent years by several other

laboratory analyses. Most important in newer studies is the inclusion of more complete perturbation models and higher quality laboratory spectra. For our line lists, we have used the data of Ross *et al.* (1988) for the wavelength range 5400 – 6800Å. Redward of 7000Å we used the data of Johns *et al.* (1976) and of Huet *et al.* (1996), with updates by Hadj Bachir *et al.* (1999). From 6800–7000Å (the (0,2,0)–(0,0,0) and (0,1,0)–(0,0,0) bands), the data of Dressler and Ramsay and Johns *et al.* (1976) are most complete, so we use these two lists preferentially in that region. For regions blueward of 5400Å, the Dressler and Ramsay wavelengths are really the only data in existence; we used their wavelengths in this blue region.

Since NH₂ has the perturbations and the bent state, modern works prefer to use the bent notation for the vibronic structure. This is in contrast with the work of Dressler and Ramsay and Johns *et al.*, in which the vibronic states were denoted in the linear notation. In our line lists, we have converted all of the vibronic notation from the linear to the bent notation. In the linear notation, sub-bands were denoted by Σ, Π, Δ, Φ, and Γ (for K= 0, ±1, ±2, ±3, ±4 respectively). To convert from a linear to a bent notation, one uses the formula

$$v^{lin} = 2v^{bent} + |l|$$

where $l = K \pm \Lambda$. Thus, the old notation for the band around 6500Å would have been (0,8,0) Π or (0,8,0) Φ, while now those bands are denoted (0,3,0) and (0,2,0) respectively [in these examples the lower level is assumed to be (0,0,0)]. Despite the fact that the linear notation has been exclusively in use by the comet community, we feel it is more appropriate to adopt the same notation as the physicists who measure these molecules.

3.6 CH⁺

The CH⁺ lines which are seen in cometary spectra are from a $A^1\Pi - X^1\Sigma^+$ transition which contains P, Q and R branches. The line list used for these bands was from Douglas and Herzberg (1942). The bands degrade towards the red. We only see lines of the 0–0 branch with relatively low J-values. While we see very few CH⁺ lines in our spectra, they are visible in both the optocenter and the tail spectra.

3.7 CO⁺

There are three band systems which can be attributed to the CO⁺ molecule. These are the first negative carbon bands ($B^2\Sigma - X^2\Sigma^+$), which occur in the UV, the comet-tail bands ($A^2\Pi - X^2\Sigma^+$), occurring in the violet through red, and the Baldet-Johnson bands ($B^2\Sigma^+ - A^2\Pi$) also in the violet. Observations in the optical bandpass do not include the first negative carbon bands (however, UV observers can find wavelengths for these lines in Rao (1950a)). Rao (1950b) showed that previous optical band assignments were in error and that the Baldet-Johnson system was much weaker than the comet-tail bands. Thus, we adopted the band assignments of Rao (1950b) for the comet-tail bands and neglected the Baldet-Johnson system entirely.

For our comet-tail line list, we used four references: Coster *et al.* (1932), Schmid and Gerö (1933), Rao (1950b) and Haridass *et al.* (2000). We updated the band designations of the first two references with the designations in Table 2 of Rao and also corrected the values for N in these papers as outlined by Rao. Unlike for CH⁺ and H₂O⁺, the CO⁺ lines could not be detected in the optocenter spectra. These were entirely found in the tail spectrum. Indeed, we detected only the 2–0 band of CO⁺ in the de Vico tail spectrum.

It is unusual to detect the 2–0 band without the 3–0 band since the 3–0 band is normally the strongest CO⁺ band in cometary spectra. The ion tail of de Vico was generally quite narrow so it is possible that our “tail” spectrum missed the strongest emissions, accounting for the weakness of the CO⁺ emissions.

3.8 H₂O⁺

With H₂O being the dominant ice in the cometary nucleus, it is not surprising to see H₂O⁺ emission in the ion tail spectrum of a comet. The electronic transition is $\tilde{A}^2 A_1 - \tilde{X}^2 B_1$, which is observed from 4000–7500Å. Much of the structure of the H₂O⁺ molecule is similar to that of the NH₂ molecule, including the strong Renner-Teller effect.

The most complete reference for the wavelengths of the H₂O⁺ lines is Lew (1976). In this paper, the bands are denoted in the linear notation (see the section on NH₂) whereas the bent notation is considered correct by current standards. Therefore, we have converted the H₂O⁺ bands to the bent notation in a manner which is identical to the NH₂.

As with the CH⁺, the H₂O⁺ lines are apparent in both the optocenter and the tail spectra. We required that a line be visible in the tail spectrum before we attributed it to H₂O⁺.

3.9 Night Sky Emission Lines

Finally, even at the high spectral resolving power of our spectra, coupled with the small entrance slit, one does end up observing emission lines produced in the Earth’s atmosphere. These lines must be accounted for when identifying lines. Fortunately, a high-resolution atlas of night sky emission lines has recently been compiled by Osterbrock *et al.* (1996) for just this purpose. The dominant molecular emission comes from OH, with contributions of O₂ and some atomic lines. We have applied a Doppler shift equal to $-\dot{\Delta}$ to the Osterbrock *et al.* wavelengths to compensate for correcting the cometary spectra to the laboratory rest frame. We confirmed that the correct Doppler shift was applied by checking the strong night sky atomic lines (Na D, O (¹D) and H α).

In the lists of identified lines which follow, we do not include the night sky lines, though they are represented on our plots. We have drawn no conclusions about their existence in our spectra, assuming they are all present. Instead, an otherwise unidentified line which is coincident with a night sky line is considered to be that night sky line without taking into account the line’s strength. Some unidentified cometary and night sky lines could, however, be coincident.

3.10 Additional Molecules

The molecules which have been identified above are the same ones which Brown *et al.* (1996) found in their spectra and which previous authors have identified. Brown *et al.* also investigated a range of other molecules which did not show up in their spectra and we have assumed they are not in our spectra either.

There are some potential molecules which we checked but our investigations proved inconclusive. One is H₂O, which is the dominant molecule in cometary nuclei and which has many transitions in our spectral region. The wavelengths of these lines are well known. However, though we started out examining our spectra for H₂O lines, we quickly realized that it would be implausible that we could detect these lines in our spectra when the Earth's atmosphere is so full of H₂O.

Another potential molecule in cometary spectra is N₂. Again, the atmosphere of the Earth makes this molecule impossible to study, so we did not search for it.

One molecule for which we searched was N₂⁺. Cochran *et al.* (2000) showed that this molecule was not present in spectra of de Vico or Hale-Bopp and placed stringent upper limits on its presence.

4 Line Identifications

Once the molecular line lists were compiled, it was necessary to examine all of the spectral orders and determine which lines we detected. First, we scrutinized our spectra for wavelength coincidences of the emission features and lines in the line lists. The strongest lines are quite easy to see in the spectra, but the weakest lines needed verification. We utilized spectra from both nights to test the veracity of a detection of a weak line. We required that the line be in both night's spectra before we would categorize the feature as a detection. Our very high signal/noise, coupled with having multiple spectra, allowed for the detection of some very weak features.

With the density of the lines in some of these bands and in our spectra, it is expected that there will be some coincidences which are accidental. When a line from the line list was coincident with an emission line, we checked to determine whether detection of the line made sense. This criterion took the form of requiring that the lines originating from lower energy levels be observed before believing that lines from higher energy transitions were detected. This is equivalent to assuming that the upper level populations can be described by some sort of effective Boltzmann temperature, which is not necessarily a physical temperature. Indeed, because C₂ is a homonuclear molecule, with no allowed dipole transition, high-J levels can be quite strong because these levels get "pumped up". This criterion was applied on a band-by-band basis. Thus, there were times when an "obvious" detection was deemed accidental because lines with lower excitation energies for the same band were not seen. We would then eliminate these accidental detections from our list.

Conversely, there are some times when we included a line, though it is not very obvious, because it is more favorable energetically than lines which were detected. A possible cause for the

absence of an expected line is coincidence with a solar absorption feature.

For the ions, we checked the tail spectrum as well as the optocenter spectra in order to determine if a line was ionic in nature. A simple coincidence of the ionic species wavelength to a feature in the optocenter spectra was not considered sufficient evidence that a line was an ion. The line also had to be present in the tail spectrum. As noted above, the CH^+ and H_2O^+ lines were observed in both the optocenter and tail spectra, but the CO^+ was only observed in the tail spectrum. It was considered sufficient to identify an ionic line if it occurred solely in the tail spectrum.

We compared our tail spectrum of de Vico with the list of identified and unidentified species in the spectrum of the tail of comet C/1996 B2 (Hyakutake) (Wyckoff *et al.* 1999). Some of Wyckoff *et al.*'s H_2O^+ lines are seen in our spectra, while others are not, and we detect many H_2O^+ lines that they did not see (however, our data are at much higher spectral resolution and so exact matches in wavelength with their identifications are difficult). We cannot confirm most of their lines; though a few of their lines other than H_2O^+ might be coincident with features in the de Vico tail spectrum, these features are generally also coincident with neutral lines identified in the optocenter spectra. The Hyakutake tail spectrum of Wyckoff *et al.* was obtained at larger distances from the nucleus than was our de Vico tail spectrum, which may explain why we do not see the same lines. In addition, with the high airmass of observations and a relatively small slit on our instrument, we could have missed the densest part of the ion tail (we do see some ions though). However, the explanation could as easily be that de Vico does not have a very strong tail spectrum.

In the blue part of the spectrum, there was an increasing wavelength overlap between the echelle orders as the wavelength decreased (higher order number). This allowed for the comparison of many lines in two different echelle orders. In general, we found the agreement excellent, with wavelength matches of $\sim 0.01 \text{ \AA}$ or better. However, for the bluest orders, the spectral overlap regions were falling well off the blaze of the grating and, consequently, became noisy in the bluest quarter of these orders. Therefore, we gave priority for identification of lines in the overlap regions to the red end of one order over the blue end of the next lowest (and therefore redder) numbered order.

One interesting result of our identifications comes from the C_2 Swan bands, particularly the $\Delta v = -1, 0,$ and 1 bands. We observe lines with very high J-values, up to $J=109!$ However, the lowest few J-value lines are missing or very weak. This is probably indicative of two different rotational temperatures for C_2 , though we have not modeled these lines yet to demonstrate this. Such an effect was also seen by Lambert *et al.* (1990) for comet Halley.

For the CN red system, we found that for a particular J level, the P_{12} and R_{12} lines were generally quite weak when compared with the P, R or Q lines of the same J level. Inspection of the line strengths in the laboratory work of Davis and Phillips (1963) shows that this is generally seen for this molecule and is normal.

In addition to the molecular emission lines, we found three atomic emission lines in the spectrum. These are the red metastable oxygen doublet, O (^1D) 6300\AA and 6364\AA , and H α . The green oxygen line at 5577\AA is cloaked by the 1–2 C_2 emission band; the Na “D” doublet is in the

wavelength region of the $C_2 \Delta v = -2$ bands. However, at most, there is just a weak hint of the cometary Na features at appropriate wavelengths. The weakness of any Na emission in de Vico is quite unusual in a comet at de Vico's heliocentric distance.

Finally, when we had exhausted our line lists, we still had a great many emission lines in our spectra with no identifications. We have flagged these in our line lists with the tag "Unid" next to the measured wavelengths and computed vacuum frequencies. A few of these "unidentified" lines are probably isotopic lines, e.g. ^{13}CN vs. ^{12}CN . Isotopic lines are quite weak but we do know of several in our spectra. However, we have chosen to ignore them for now, because proper identification takes modeling the band in question, which is beyond the scope of this atlas.

Figure 1 shows a plot of the blue half of order 49, covering the wavelength range from 6957–7014Å. In this figure, we show spectra from both nights, offset from one another for clarity. The spectra are plotted with an expanded y axis in order to illustrate the weaker features. The spectra are plotted in three panels to allow for inspection of the features. Plotted below the spectra are tick marks for all of the identified lines, in this case lines of CN, C_2 , NH_2 and H_2O^+ . Plotted above the spectra are tick marks for the night sky OH (Doppler shifted to the appropriate rest frame for the comet) and the position of lines we could not identify. Dashed vertical lines mark the position of the features in the spectra. Examination of Fig. 1 shows that there are a substantial number of quite strong lines which are unidentified, including lines with more than 20,000 counts!

In contrast, Figure 2 shows order 77 from 4 October. There are obvious emission features (and solar absorptions) in this spectrum. Indeed, we have located 64 lines in this spectral region which are visible in spectra from both nights. However, we can not identify the molecule for any of these 64 features. This order is an excellent example of the desperate need for more laboratory studies.

Figure 3 shows a plot of all of our detected lines, by molecule, as a function of wavelength. Unidentified features are also marked. The gaps which can be seen in the red for molecules such as C_2 and CN are the result of the interorder gaps in our spectra. Molecules such as C_2 and NH_2 can be found at almost any optical wavelength, while C_3 and CH are confined to the blue.

Table III gives a representative listing of the identifications for the wavelength region from 6957–6976Å, the spectral region shown in the top panel of Fig. 1. A table similar to Table III for each of the molecules shown in Figure 3 is available in digital (ASCII text) form¹. These tables contain the wavelength and vacuum frequency of the lines, along with the band designations and transition. A table of the unidentified lines is also available in digital form. We also will make available a table of all of the identified and unidentified features, sorted by wavelength.

As with Table III, the digital tables will be entirely in ASCII characters and will not use any sub- or super-scripts; they can be utilized on any computer without having to deal with embedded special characters. The tables are in fixed format. For most molecules, the electronic transitions are listed by their letter designations (A, B, X) instead of their term designations. For C_2 , we use the more common names of Swan and Phillips, where the Swan band is the $d^3\Pi_g - a^3\Pi_u$ band

¹These tables and the plots mentioned below may be obtained from the web site (currently pdssbn.astro.umd.edu) of the Small Bodies Node of the NASA Planetary Data System

and the Phillips is the $A^1\Pi_u - X^1\Sigma_g^+$ band. As vibrational transitions carry designations with different forms for diatomic and polyatomic molecules, those transitions are listed in the manner appropriate for each molecule. In all cases, the upper state is listed first, then the lower state. For the rotational transitions, the designations are very dependent on the individual molecule, since some just have P, Q and R branches, some, such as CN A-X, have branches such as P₁₂, and some, such as CH, have branches such as $^RQ_{21}fe$ (which is listed as “[^]RQ21fe” in plain ASCII). Molecules such as NH₂ and H₂O⁺ have rotational states which are designated with three quantum numbers of the form $N'_{K'_a K'_c} - N''_{K''_a K''_c}$. The NH₂ and H₂O⁺ rotational states are separated into F₁ and F₂ components. We have not included those designations in our tables.

Sometimes more than one transition occurs at the same frequency. We list all rotational transitions from the same vibrational and electronic band on the same line in the tables. When there are concurrent transitions from different vibrational bands, we list the two different band transitions on separate lines of the table.

We chose to list only the wavelength and frequency of the unidentified lines and not their strengths. There were several reasons behind this decision. First, we have no absolute flux calibration of these coude spectra so there is no way to calibrate the blaze function. Additionally, we have not attempted to remove the atmospheric extinction and the comet was observed at an airmass of 2–3 airmasses. This means that relative strengths within an order are probably accurate, but order-to-order comparisons are less meaningful. We have made no attempt to model the Swings effect for any molecule. Without such a model, any line could be a different strength than expected from laboratory measurements. Also, the lines are often highly blended. Thus, to determine line strengths a full deconvolution model must be computed. For the over 4000 unidentified lines this is a huge undertaking. Such an exercise should be done for individual studies, but are not realistic for this atlas.

In addition to the tables of identified and unidentified features, we are making available PostScript files of plots of our spectra in two formats. The first format is plots similar to Fig. 1. For each order, there are two plots, each with 3 panels, showing two spectra and the identified and unidentified lines. These are all plotted with expanded y scales to show the weaker features. The features are marked in color, as with Fig. 1. The colors of the markers remain the same for each molecule across all plots. That is, there is space and a color allocated for each molecule even when that molecule is not present in a particular order. Included in these plots are the ionic species CH⁺ and H₂O⁺, since they are visible in the optocenter spectra. The CO⁺ only shows up in order 81 in the tail spectrum. This spectrum is shown in Fig. 2 of Cochran *et al.* (2000) with the CO⁺ and CH⁺ identified.

The second form of plot which we are making available is the spectra without expansion of the y axis. These plots take the form of four panel plots with two orders per plot (each of two panels). Each panel is scaled in y to fit the maximum strength line in that panel. These plots are a valuable adjunct to the identification plots because they show the relative strength of the strong and weak lines. They also allow for the inspection of the telluric absorption features which plague some orders.

It is quite likely that there are a few real features which we have missed in our tabulations

because the sheer quantity of data makes such misses inevitable. Indeed, every time we have inspected the plots of identifications, we have found an additional line or two. There are some lines which we may have located which may be less believable to a reader. Sometimes our choice to include these lines in our lists comes from our ability to manipulate the spectra digitally and to change the scaling to view a feature better; sometimes we may have overactive imaginations! There are times when an identified molecular line seems slightly off in wavelength from the peak of a feature. We have assumed that it is possible that the wavelengths of the laboratory line lists are not always entirely accurate. Additionally, in regions where lines are blended, or in the regions of strong telluric absorption features, the observed line center may be shifted from a laboratory value. This is true also for our measured positions of unidentified features. Therefore, it is imperative that a user of these data inspect the full scale plots for context and for absorptions and that they examine the feature plots for blending. Users who wish to model the unidentified features should contact us for access to the data, so that the lines can be properly deblended.

5 Summary

In 1995, we obtained high spectral resolution observations of the dust-poor comet 122P/de Vico at McDonald Observatory. We have compiled many laboratory studies of molecules thought to be present in the spectra of comets and have used these to identify 12,219 lines in the spectrum of de Vico. In addition, we found 4,055 lines we could not attribute to a particular molecule. We found emission lines of five neutral radicals: 6862 were of C_2 , 1282 of C_3 , 1167 of CN , 169 of CH , and 2569 of NH_2 . We also identified three atomic lines. We observed three ionic species: 129 lines of H_2O^+ , 11 lines of CH^+ and 27 lines of CO^+ . The CO^+ can only be seen in the spectrum obtained 100 arcsec tailward, while the H_2O^+ and CH^+ can be seen in both the tail and optocenter spectra.

Our lists of identified and unidentified emission lines are available in digital format from the Planetary Data System Small Bodies Node. In addition, we are making available annotated plots of high resolution spectra of a comet, covering almost the complete optical bandpass. The line lists, coupled with the plots, should prove to be an invaluable tool for future studies of high resolution cometary spectra. Only by first identifying the molecules which are present in a spectrum can the important chemical analyses be performed.

Acknowledgments

This work was funded by NASA Grant NAG5 9003. We are indebted to Dr. Claude Arpigny for encouragement and many helpful discussions. We thank Dr. Eric Bakker for pointers to several of the line lists. We thank Dr. Tony Farnham for a careful reading of the manuscript. We are particularly indebted to the various people who made digital line lists available, either at our requests or as part of a database attached to a paper. These include Drs. Balfour, Brown, Davis, Destombes, Haridass, Jørgensen, Kurucz, Osterbrock, and Ross.

References

- BALFOUR, W. J., J. CAO, C. V. V. PRASAD, AND C. X. W. QIAN 1994. Laser-induced fluorescence spectroscopy of the $\tilde{A}^1\Pi_u - \tilde{X}^1\Sigma_g^+$ transition in jet-cooled C_3 . *J. Chem. Phys.* **101**, 10343–10349.
- BALLIK, E. A. AND D. A. RAMSAY 1967. An extension of the Phillips system of C_2 and a survey of C_2 states. *Astrophys. J.* **137**, 84–101.
- BROWN, M. E., A. H. BOUCHEZ, H. SPINRAD, AND C. M. JOHNS-KRULL 1996. A high-resolution catalog of cometary emission lines. *Astron. J.* **112**, 1197–1202.
- CHAUVILLE, J., J. P. MAILLARD, AND A. W. MANTZ 1977. The infrared part of the C_2 Phillips system (2.3–0.9 μ m). *J. Mol. Spec.* **68**.
- COCHRAN, A. L., W. D. COCHRAN, AND E. S. BARKER 2000. N_2^+ and CO^+ in comets 122P/1995 S1 (deVico) and C/1995 O1 (Hale-Bopp). *Icarus* **146**, 583–593.
- COSTER, D., H. BRONS, AND H. BULTHUIS 1932. Das bandenspektrum des CO^+ . *Zeit. f. Physik* **79**, 787–822.
- DAVIS, S. P. AND J. G. PHILLIPS 1963. *The Red System (A-X) of the CN Molecule*. University of California Press, Berkeley and Los Angeles.
- DOUGLAS, A. E. AND G. HERZBERG 1942. Band spectrum and structure of the CH^+ molecule: Identification of three interstellar lines. *Can. J. Res.* **20A**, 71–82.
- DRESSLER, K. AND D. A. RAMSAY 1959. The electronic absorption spectra of NH_2 and ND_2 . *Phil. Trans. Roy. Soc. London A* **251**, 553–602.
- GAUSSET, L., G. HERZBERG, A. LAGERQVIST, AND B. ROSEN 1965. Analysis of the 4050- \AA group of the C_3 molecule. *Astrophys. J.* **142**, 45–76.
- HADJ BACHIR, I., T. R. HUET, J.-L. DESTOMBES, AND M. VERVLOET 1999. A combined analysis of laser optogalvanic and fourier transform emission spectra of NH_2 near its barrier to linearity. *J. Mol. Spec.* **193**, 326–353.
- HARIDASS, C., C. V. V. PRASAD, AND S. PADDI REDDY 2000. The comet-tail ($A^2\Pi_i - X^2\Sigma^+$) system of $^{12}C^{16}O^+$: A reinvestigation. *J. Mol. Spec.* **199**, 180–187.
- HUET, T. R., I. HADJ BACHIR, H. BOLVIN, A. ZELLAGUI, J. L. DESTOMBES, AND M. VERVLOET 1996. NH_2 transitions of cometary interest in the near infrared. *Astron. Astrophys.* **311**, 343–346.
- JOHNS, J. W. C., D. A. RAMSAY, AND S. C. ROSS 1976. The $\tilde{A}^2A_1 - \tilde{X}^2B_1$ absorption spectrum of NH_2 between 6250 and 9500 \AA . *Can. J. Phys.* **54**, 1804–1814.
- JØRGENSEN, U. G. AND M. LARSSON 1990. Molecular opacities of astrophysical interest: The $A^2\Pi - X^2\Sigma^+$ system of CN. *Astron. Astrophys.* **238**, 424–434.

- JØRGENSEN, U. G., M. LARSSON, A. IWAMAE, AND B. YU 1996. Line intensities for CH and their application to stellar atmospheres. *Astron. Astrophys.* **315**, 204–211.
- KURUCZ, R. L. 1995. The Kurucz Smithsonian atomic and molecular database. In *Astrophysical Applications of Powerful New Databases* (S. J. Adelman and W. L. Wiese, Eds.) pp. 205–210 ASP Conference Series Vol. 78.
- LAMBERT, D. L., Y. SHEFFER, A. C. DANKS, C. ARPIGNY, AND P. MAGAIN 1990. High-resolution spectroscopy of the C₂ Swan 0–0 band from comet P/Halley. *Astrophys. J.* **353**, 640–653.
- LEW, H. 1976. Electronic spectrum of H₂O⁺. *Can. J. Phys.* **54**, 2028–2049.
- MERER, A. J. 1967. Absorption spectra of C₃ and C₃H₂ from the flash photolysis of diazopropyne. *Can. J. Phys.* **45**, 4103–4111.
- OSTERBROCK, D. E., J. P. FULBRIGHT, A. R. MARTEL, M. J. KEANE, AND S. C. TRAGER 1996. Night-sky high-resolution spectral atlas of OH and O₂ emission lines for echelle spectrograph wavelength calibration. *Pub. Astron. Soc. Pac.* **108**, 277–308.
- PHILLIPS, J. G. AND S. P. DAVIS 1968. *I. The Swan System of the C₂ Molecule. II. The Spectrum of the HgH Molecule.* University of California Press, Berkeley and Los Angeles.
- RAO, K. N. 1950a. The band spectrum of CO⁺. I. First negative system (B Σ – X²Σ). *Astrophys. J.* **111**, 50–59.
- RAO, K. N. 1950b. The band spectrum of CO⁺. II. Comet-tail system (A Π – X²Σ). *Astrophys. J.* **111**, 306–313.
- ROSS, S. C., F. W. BIRSS, M. VERVLOET, AND D. A. RAMSAY 1988. The absorption spectrum of NH₂ in the region 5300 to 6800Å. *J. Mol. Spec.* **129**, 436–470.
- SCHMID, R. AND GERÖ 1933. Zur rotationsanalyse der ²Σ → ²Σ⁻ und ²Π → ²Σ⁻ banden des CO⁺. *Zeit. f. Physik* **86**, 297–313.
- TOKARYK, D. W. AND D. E. CHOMIAK 1997. Laser spectroscopy of C₃: Stimulated emission and absorption spectra of the $\tilde{A}^1\Pi_u - \tilde{X}^1\Sigma_g^+$ transition. *J. Chem. Phys.* **106**, 7600–7608.
- TULL, R. G., P. J. MACQUEEN, C. SNEDEN, AND D. L. LAMBERT 1995. The high-resolution cross-dispersed echelle white-pupil spectrometer of the McDonald Observatory 2.7m telescope. *Pub. Astron. Soc. Pac.* **107**, 251–264.
- VALK, J. H., C. R. O'DELL, A. L. COCHRAN, W. D. COCHRAN, C. B. OPAL, AND E. S. BARKER 1992. Near-ultraviolet spectroscopy of comet Austin (1989c₁). *Astrophys. J.* **388**, 621–632.
- WYCKOFF, S., R. S. HEYD, AND R. FOX 1999. Unidentified molecular bands in the plasma tail of comet Hyakutake (C/1996 B2). *Astrophys. J.* **512**, L73–L76.
- ZHANG, H. W., G. ZHAO, AND J. Y. HU 2001. A catalogue of emission lines in spectra of comet C/1995 O1 (Hale-Bopp). *Astron. Astrophys.* **367**, 1049–1055.

Table I: Log of Observations

File #	Date (UT)	Start Time (UT)	Exposure (sec)	Δ (AU)	$\dot{\Delta}$ (km/sec)	R_h (AU)	\dot{R}_h (km/sec)
RV23200	03 Oct 95	11:37:30	600	1.00	-14.3	0.66	-2.9
RV23201	03 Oct 95	11:57:17	600	1.00	-14.3	0.66	-2.9
RV23257	04 Oct 95	11:10:49	1500	0.99	-12.9	0.66	-1.7
RV23258 ^a	04 Oct 95	11:42:21	1200	0.99	-12.9	0.66	-1.7

Note: a) 100 arcsec tailward

Table II: Wavelengths Observed

Order	Start (\AA)	End (\AA)	Order	Start (\AA)	End (\AA)	Order	Start (\AA)	End (\AA)
89	3829.77	3893.62	70	4869.76	4950.90	51	6684.03	6795.33
88	3873.32	3937.89	69	4940.35	5022.66	50	6817.70	6931.23
87	3917.88	3983.19	68	5013.01	5096.53	49	6956.83	7072.67
86	3963.46	4029.53	67	5087.84	5172.60	48	7101.75	7220.00
85	4010.12	4076.96	66	5164.94	5250.98	47	7252.84	7373.60
84	4057.89	4125.53	65	5244.41	5331.77	46	7410.50	7533.88
83	4106.81	4175.26	64	5326.36	5415.08	45	7575.16	7701.29
82	4156.91	4226.20	63	5410.91	5501.04	44	7747.31	7876.30
81	4208.26	4278.40	62	5498.18	5589.76	43	7927.46	8059.45
80	4260.88	4331.90	61	5588.32	5681.40	42	8116.19	8251.32
79	4314.84	4386.75	60	5681.46	5776.09	41	8314.13	8452.55
78	4370.18	4443.01	59	5777.75	5873.98	40	8521.97	8663.85
77	4426.96	4500.73	58	5877.37	5975.26	39	8740.46	8885.98
76	4485.23	4559.97	57	5980.48	6080.08	38	8970.45	9119.79
75	4545.05	4620.78	56	6087.27	6188.65	37	9212.88	9366.25
74	4606.48	4683.24	55	6197.94	6301.16	36	9468.77	9626.40
73	4669.60	4747.41	54	6312.71	6417.84	35	9739.28	9901.42
72	4734.47	4813.35	53	6431.82	6538.93	34	10025.71	10192.61
71	4801.16	4881.16	52	6555.50	6664.66			

Table III: The Lines of Order 49, panel 1

Wavelength (Å)	Frequency (cm ⁻¹)	Molecule	Electronic ¹ Transition	Vibrational ² Transition	Rotational ³ Transitions
6956.831	14370.397	H2O+	A-X	(0,2,0) - (0,0,0)	3 1 2 - 2 0 2
6957.301	14369.430	CN	A-X	3-0	P1(2)
6957.612	14368.780	CN	A-X	3-0	P2(9)
6957.731	14368.540	CN	A-X	3-0	Q1(8) R1(19)
6958.122	14367.730	NH2	A-X	(0, 2,0) - (0,0,0)	5 1 5 - 5 0 5
6958.228	14367.513	H2O+	A-X	(0,2,0) - (0,0,0)	3 1 2 - 2 0 2
6958.640	14366.655	Unid			
6958.864	14366.200	C2	Phil	4-0	Q(18)
6958.907	14366.110	CN	A-X	3-0	P1(3)
6959.100	14365.710	CN	A-X	3-0	Q2(14)
6959.394	14365.100	CN	A-X	3-0	Q1(9)
6960.547	14362.730	CN	A-X	3-0	R1(20)
6960.805	14362.190	CN	A-X	3-0	P1(4)
6960.850	14362.100	NH2	A-X	(0, 2,0) - (0,0,0)	5 1 5 - 5 0 5
6961.318	14361.130	CN	A-X	3-0	Q1(10)
6961.720	14360.312	Unid			
6961.903	14359.930	CN	A-X	3-0	P2(10)
6962.377	14358.950	C2	Phil	4-0	P(14)
6962.795	14358.090	CN	A-X	3-0	P12(3) Q2(15)
6962.955	14357.760	CN	A-X	3-0	P1(5)
6963.331	14356.983	H2O+	A-X	(0,2,0) - (0,0,0)	2 1 1 - 1 0 1
6963.496	14356.640	CN	A-X	3-0	Q1(11)
6963.569	14356.490	CN	A-X	3-0	R1(21)
6963.594	14356.440	NH2	A-X	(0, 2,0) - (0,0,0)	4 1 4 - 4 0 4
6963.880	14355.862	Unid			
6964.080	14355.447	Unid			
6964.303	14354.980	NH2	A-X	(0, 2,0) - (0,0,0)	1 1 1 - 1 0 1
6964.590	14354.394	Unid			
6964.800	14353.961	Unid			
6965.392	14352.740	CN	A-X	3-0	P1(6)
6965.470	14352.575	H2O+	A-X	(0,2,0) - (0,0,0)	2 1 1 - 1 0 1
6965.901	14351.690	CN	A-X	3-0	Q1(12)
6966.064	14351.350	NH2	A-X	(0, 2,0) - (0,0,0)	5 1 4 - 4 2 2
6966.200	14351.070	C2	Phil	4-0	R(26)
6966.212	14351.050	CN	A-X	3-0	P12(4)
6966.326	14350.810	NH2	A-X	(0, 2,0) - (0,0,0)	4 1 4 - 4 0 4
6966.452	14350.550	CN	A-X	3-0	P2(11)
6966.637	14350.170	NH2	A-X	(0, 2,0) - (0,0,0)	2 1 2 - 2 0 2
6966.700	14350.040	NH2	A-X	(0, 2,0) - (0,0,0)	3 1 3 - 3 0 3
6966.719	14350.000	CN	A-X	3-0	Q2(16)
6967.060	14349.305	Unid			

Table III (cont.)

Wavelength (Å)	Frequency (cm ⁻¹)	Molecule	Electronic ¹ Transition	Vibrational ² Transition	Rotational ³ Transitions
6967.380	14348.646	Unid			
6967.730	14347.909	Unid			
6967.904	14347.560	NH ₂	A-X	(0, 2,0) - (0,0,0)	5 1 4 - 4 2 2
6968.061	14347.240	CN	A-X	3-0	P1(7)
6968.260	14346.832	Unid			
6968.584	14346.160	CN	A-X	3-0	Q1(13)
6968.760	14345.798	Unid			
6969.124	14345.050	C ₂	Phil	4-0	Q(20)
6969.396	14344.490	NH ₂	A-X	(0, 2,0) - (0,0,0)	3 1 2 - 2 2 0
6969.993	14343.260	NH ₂	A-X	(0, 2,0) - (0,0,0)	3 1 3 - 3 0 3
6970.001	14343.240	CN	A-X	3-0	P12(5)
6970.152	14342.934	H ₂ O+	A-X	(0,2,0) - (0,0,0)	1 1 0 - 0 0 0
6970.499	14342.220	NH ₂	A-X	(0, 2,0) - (0,0,0)	1 1 1 - 1 0 1
6970.846	14341.500	CN	A-X	3-0	Q2(17)
6970.892	14341.410	NH ₂	A-X	(0, 2,0) - (0,0,0)	2 1 2 - 2 0 2
6971.032	14341.120	CN	A-X	3-0	P1(8)
6971.181	14340.820	CN	A-X	3-0	P2(12)
6971.513	14340.130	CN	A-X	3-0	Q1(14)
6971.900	14339.341	Unid			
6972.137	14338.850	NH ₂	A-X	(0, 2,0) - (0,0,0)	3 1 2 - 2 2 0
6972.600	14337.908	Unid			
6973.518	14336.010	C ₂	Phil	4-0	P(16)
6973.720	14335.596	H ₂ O+	A-X	(0,2,0) - (0,0,0)	1 1 0 - 0 0 0
6973.962	14335.100	CN	A-X	3-0	P12(6)
6974.248	14334.510	CN	A-X	3-0	P1(9)
6974.693	14333.600	CN	A-X	3-0	Q1(15)
6975.193	14332.570	CN	A-X	3-0	Q2(18)
6976.128	14330.650	CN	A-X	3-0	P2(13)

NOTES:

- 1: For C₂, "Phil" is the Phillips band (A ¹Π_u - X ¹Σ_g⁺).
- 2: The designation of the vibrational transition is different for diatomic and polyatomic molecules.
- 3: The rotational transition designations depend on the molecule.
For CN, more than one transition may be listed per line if they occur at the same wavelength.
For NH₂, rotational quantum numbers are listed as $N'_{K'_a K'_c} - N''_{K''_a K''_c}$.

6 Figure Captions

Figure 1: A representative spectral order is shown with an expanded y scale in order to demonstrate the detection of weak features. Two spectra are plotted. The bottom, black spectrum, is RV23257, from 4 October 1995. The top, blue spectrum, is RV23201, from 3 October 1995. The blue spectrum is offset vertically for clarity. Marked on the plot are all of the identified and unidentified features in the spectrum.

Figure 2: Spectral order 77 shows many strong emission features but we can not identify the molecule responsible for any of these lines. There are 64 emission lines in this spectral region.

Figure 3: The wavelengths of the detected lines of the various molecules and atoms we detected are plotted. The gaps at the red end for molecules such as C_2 are caused by the interorder gaps in our spectra. The wavelengths where we have unidentified lines are also marked.

122P/deVico Order 49 (part a)

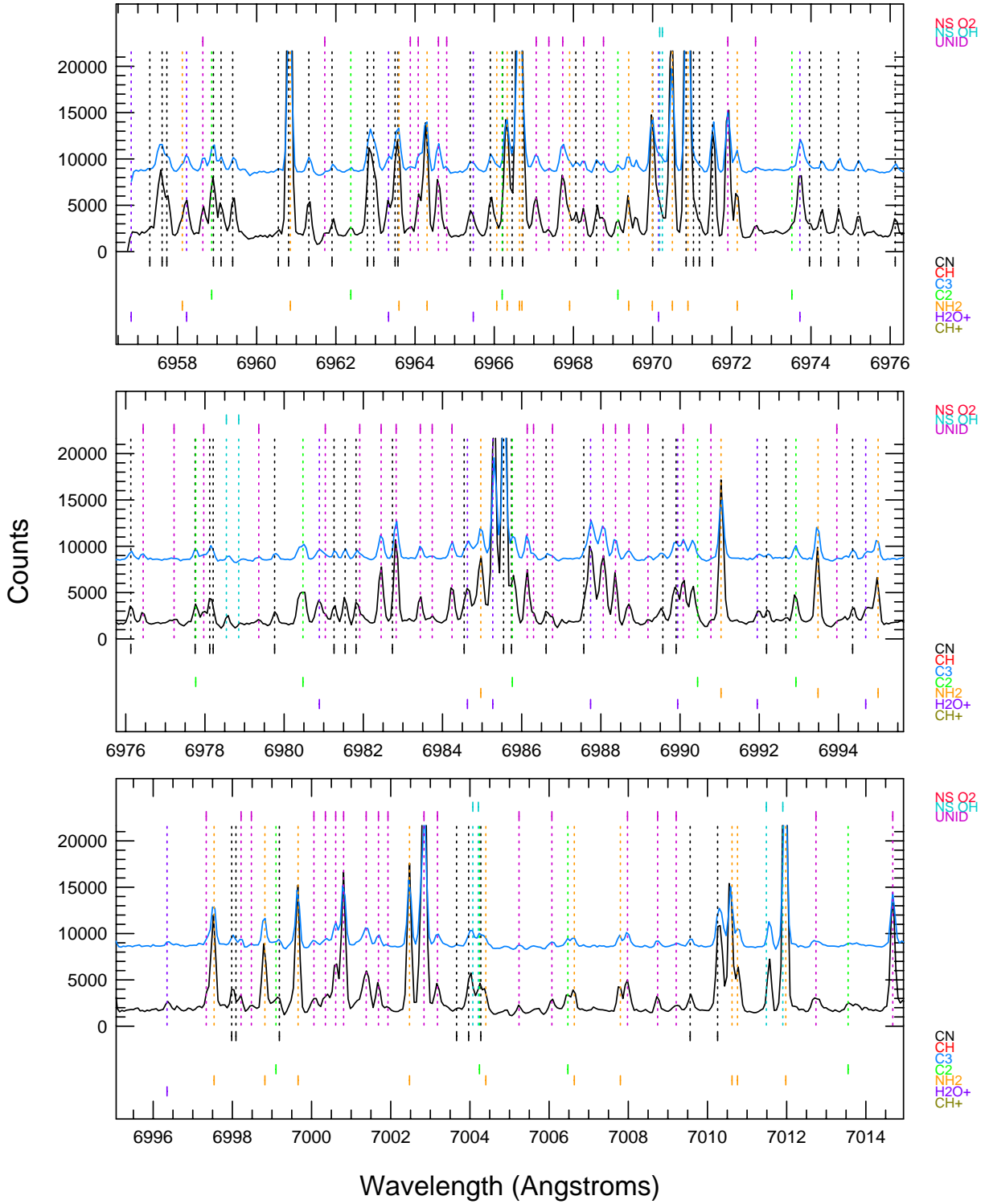


Figure 1: Cochran and Cochran 2001

122P/de Vico -- Order 77 (RV23257)

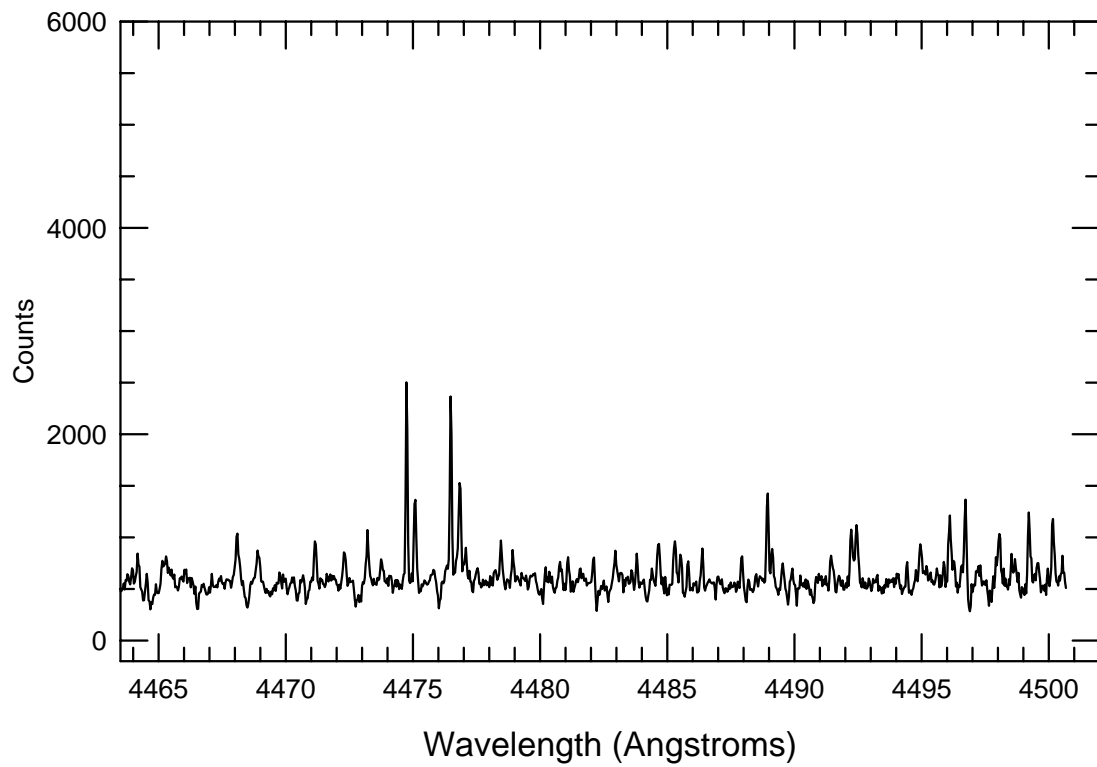
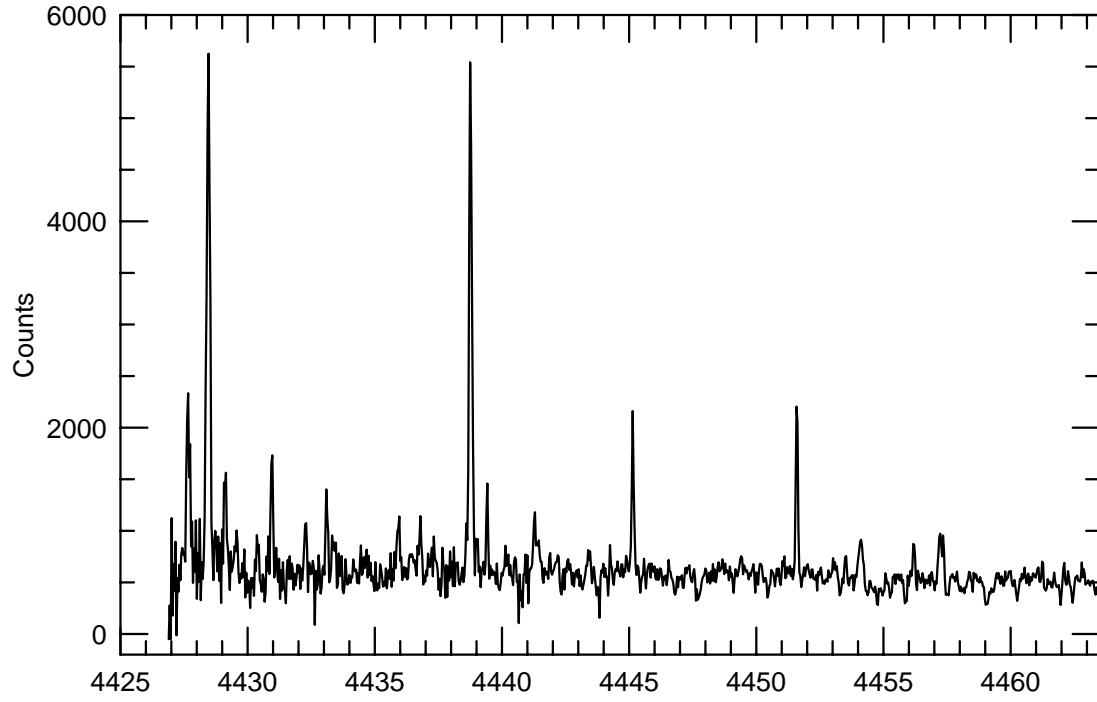


Figure 2: Cochran and Cochran 2001

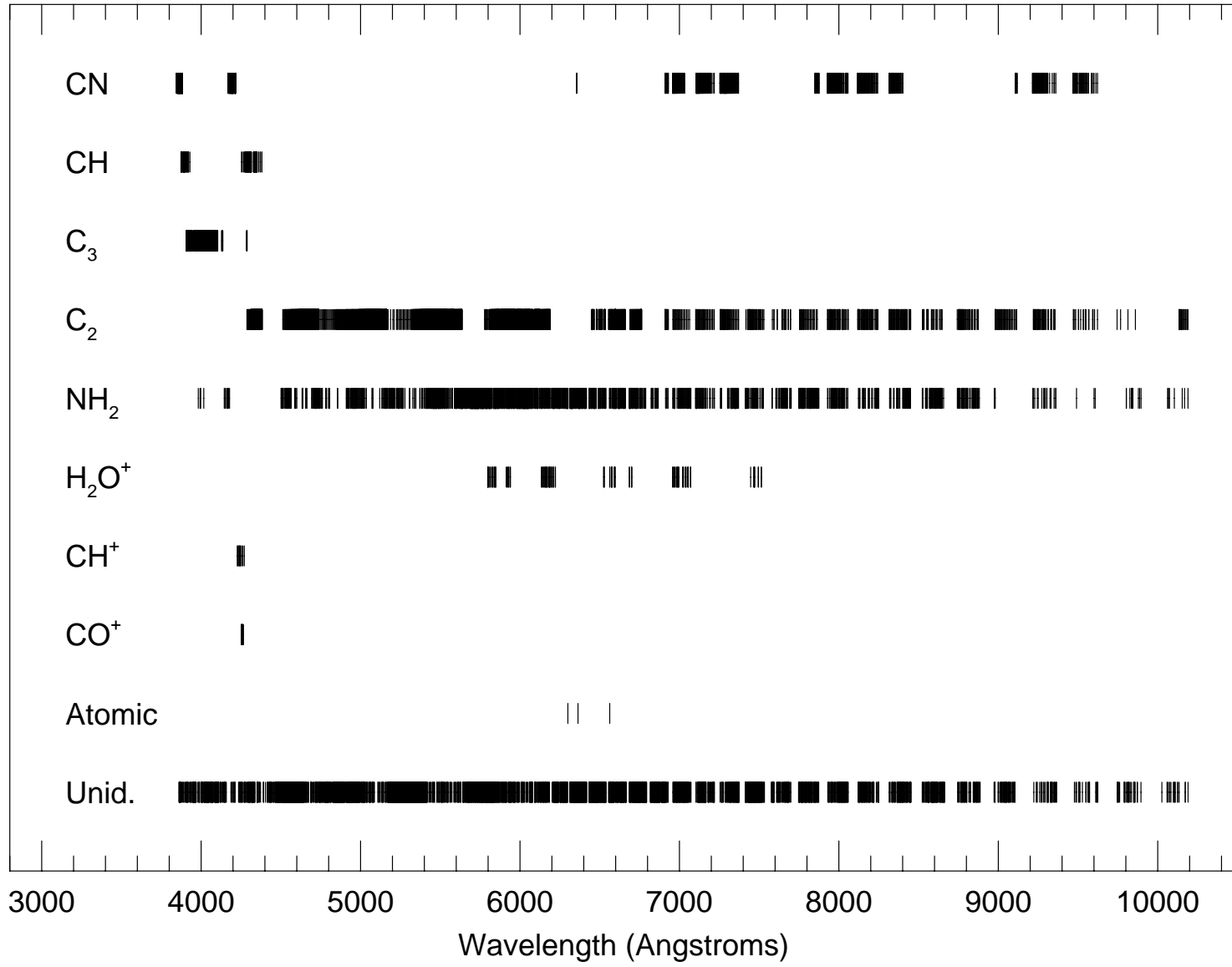


Figure 3: Cochran and Cochran 2001